Int J Fract (2007) 144:247–265
DOI 10.1007/s10704-007-9098-x

ORIGINAL PAPER

Mixed mode failure criteria for brittle elastic V-notched structures

Elad Priel · Arie Bussiba · Ilan Gilad · Zohar Yosibash

Received: 7 December 2006 / Accepted: 20 June 2007 / Published online: 24 July 2007

Abstract Three mixed mode failure initiation criteria at reentrant corners in brittle elastic materials are examined. Prediction of failure load and crack initiation angle are compared to experimental observations carried out on PMMA (polymer) and MACOR (glass ceramic) V-notched specimens. Since the mode mixity ratio influences greatly both the failure load and crack initiation angle, a detailed experimental procedure has been followed, focusing on obtaining a wide range of mode mixity ratios. It is demonstrated that by assuming a sharp V-notch tip some failure criteria predict reasonably well both the crack initiation angle and failure load.

Keywords Failure initiation · Mixed-mode · Generalized stress intensity factors · V-notch · Ceramics · p-version FEA

1 Introduction

Failure criteria for brittle materials containing V-notches of variable opening angles, multi-material interfaces or orthotropic materials have become of major interest because of failure initiation phenomena that occur in composite materials and electronic devices (see e.g. Yosibash et al. (2003)). A reliable criterion for predicting the failure initiation instance (crack formation) in these cases in the vicinity of a sharp V-notch tip, especially when a complex state of stress is present, is a topic of active research and interest (Dunn et al. 1997a; Seweryn and Lukaszewicz 2002; Yosibash et al. 2006). A crack tip is a particular case when the V-notch solid angle is 2π. For the simplified *mode I* state of stresses in the vicinity of a V-notch tip, i.e., tension perpendicular to the V-notch bi-sector alone, several failure criteria have been proposed and verified by experimental observations, see Dunn et al. (1997a), Fett (1996), Gomez and Elices (2003), Lazzarin and Zmabardi (2001), Leguillon (2002), Seweryn (1994). A comparison of several failure criteria with experimental observations was presented in Yosibash et al. (2004), demonstrating their validity.

For cracked domains under mixed mode loading several failure criteria are available as the maximum tangential stress criterion (Anderson 2005) or the strain energy density criterion (Erdogan and Sih 1963; Sih and Macdonald 1974). There are also criteria that examine the energy release rate for a kinked crack or relay on pure mixed mode empirical findings (Chang et al. 2006; Nuismer 1975; Palaniswamy and Knuass 1978).

For V-notched configurations the number of mixed mode failure initiation criteria suggested and validated via experimental observations is very limited (Dunn et al. 1997b; Seweryn and Lukaszewicz 2002; Yosibash et al. 2006). The failure criterion in Dunn et al. (1997b) is restricted to low values of mode mixity when

E. Priel · A. Bussiba · I. Gilad · Z. Yosibash (✉)
Pearlstone Center for Aeronautical Engineering Studies, Department of Mechanical Engineering, Ben-Gurion University of the Negev, Beer-Sheva 84105, Israel
e-mail: zohary@bgu.ac.il

mode I dominates and therefore is not applicable as a general mixed mode failure criterion. The criteria proposed in Seweryn and Lukaszewicz (2002), Yosibash et al. (2006), and a new simpler criterion which is an extension of the Strain Energy Density (SED) criterion presented in Yosibash et al. (2004) for mode I loading, are compared on the basis of their ability to predict failure loads and failure initiation angles. To this end experiments on V-notched specimens under mixed mode loading are conducted and reported. The paper is organized as follows: We start in Sect. 2 with notations and presentation of the elastic stress and displacement expressions in the vicinity of the V-notch tip. We then review the two failure criteria in Seweryn and Lukaszewicz (2002) and Yosibash et al. (2006), discussing their advantages and drawbacks. In Sect. 3 we introduce a new failure initiation criterion which is a generalization of the SED criterion in Yosibash et al. (2004). To validate the different failure criteria, mixed mode experiments were conducted on PMMA (polymer) and MACOR (machinable glass ceramic) V-notched specimens. The experimental data are presented in Sect. 4. Comparison of predicted failure load and crack initiation angle for a large range of experimental results (mixed mode) reported in the literature and these conducted in this study are presented in Sect. 5. We summarize in Sect. 6.

2 Notations and known mixed mode failure criteria

Consider a 2-D domain under the assumption of plane-strain having a V-notch reentrant corner shown in Fig. 1. The displacement and stress in the vicinity of a sharp V-notch tip, assuming $\boldsymbol{u}(\mathbf{0}) = \mathbf{0}$, are expressed as an asymptotic series (Yosibash et al. 2006):

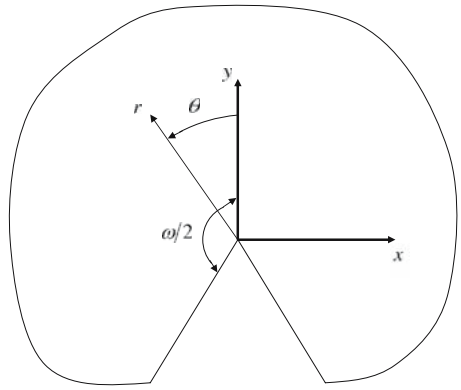

Fig. 1 Area surrounding the V-notch tip

$$\boldsymbol{u} \overset{\text{def}}{=} \begin{Bmatrix} u_r \\ u_\theta \end{Bmatrix} = \sum_{\ell=1} A_\ell r^{\alpha_\ell} \begin{Bmatrix} u_r^{(\ell)}(\theta) \\ u_\theta^{(\ell)}(\theta) \end{Bmatrix} = \sum_{\ell=1} A_\ell r^{\alpha_\ell} \boldsymbol{u}^{(\ell)}(\theta) \tag{1}$$

$$\boldsymbol{\sigma} \overset{\text{def}}{=} \begin{Bmatrix} \sigma_{rr} \\ \sigma_{\theta\theta} \\ \sigma_{r\theta} \end{Bmatrix} = \sum_{\ell=1} A_\ell r^{\alpha_\ell - 1} \begin{Bmatrix} \sigma_{rr}^{(\ell)}(\theta) \\ \sigma_{\theta\theta}^{(\ell)}(\theta) \\ \sigma_{r\theta}^{(\ell)}(\theta) \end{Bmatrix} = \sum_{\ell=1} A_\ell r^{\alpha_\ell - 1} \boldsymbol{\sigma}^{(\ell)}(\theta) \tag{2}$$

where r, θ are cylindrical coordinates located in the V-notch tip (see Fig. 1), A_ℓ is a coefficient that depends on the load called Generalized Stress Intensity Factor (GSIF), α_ℓ the eigen values and $\boldsymbol{u}^{(\ell)}(\theta)$ and $\boldsymbol{\sigma}^{(\ell)}(\theta)$ the eigen vectors, which depend on material parameters and the geometry in the vicinity of the V-notch tip.

When $r \to 0$ the first two terms dominate since $\alpha_1, \alpha_2 < 1$ and (1) is explicitly given as:

$$\begin{aligned} \boldsymbol{u}(r,\theta) &\overset{\text{def}}{=} \{u_r u_\theta\} \\ &= A_1 r^{\alpha_1} \begin{Bmatrix} \left[\cos(1+\alpha_1)\theta + \dfrac{[\lambda+3\mu-\alpha_1(\lambda+\mu)]}{(\lambda+\mu)(1-\alpha_1)} \dfrac{\sin[\omega(1+\alpha_1)/2]}{\sin[\omega(1-\alpha_1)/2]} \cos(1-\alpha_1)\theta \right] \Big/ \left(2\mu\alpha_1 \sigma_{\theta\theta}^{I}(\theta=0)\right) \\ \left[-\sin(1+\alpha_1)\theta - \dfrac{[\lambda+3\mu+\alpha_1(\lambda+\mu)]}{(\lambda+\mu)(1-\alpha_1)} \dfrac{\sin[\omega(1+\alpha_1)/2]}{\sin[\omega(1-\alpha_1)/2]} \sin(1-\alpha_1)\theta \right] \Big/ \left(2\mu\alpha_1 \sigma_{\theta\theta}^{I}(\theta=0)\right) \end{Bmatrix} \\ &+ A_2 r^{\alpha_2} \begin{Bmatrix} \left[\sin(1+\alpha_2)\theta + \dfrac{[\lambda+3\mu-\alpha_2(\lambda+\mu)]}{(\lambda+\mu)(1+\alpha_2)} \dfrac{\sin[\omega(1+\alpha_2)/2]}{\sin[\omega(1-\alpha_2)/2]} \sin(1-\alpha_2)\theta \right] \Big/ \left(2\mu\alpha_2 \sigma_{r\theta}^{II}(\theta=0)\right) \\ \left[\cos(1+\alpha_2)\theta + \dfrac{[\lambda+3\mu+\alpha_2(\lambda+\mu)]}{(\lambda+\mu)(1+\alpha_2)} \dfrac{\sin[\omega(1+\alpha_2)/2]}{\sin[\omega(1-\alpha_2)/2]} \cos(1-\alpha_2)\theta \right] \Big/ \left(2\mu\alpha_2 \sigma_{r\theta}^{II}(\theta=0)\right) \end{Bmatrix} \end{aligned} \tag{3}$$

where μ and λ are Lame's constants associated with the Young's modulus and Poisson ratio by:

$$\mu = \frac{E}{2(1+\nu)} \quad \lambda = \frac{E\nu}{(1+\nu)(1-2\nu)} \tag{4}$$

Similarly (2) is explicitly given as:

$$\boldsymbol{\sigma} = \begin{Bmatrix} \sigma_{rr} \\ \sigma_{\theta\theta} \\ \sigma_{r\theta} \end{Bmatrix} = A_1 r^{\alpha_1 - 1} \begin{Bmatrix} \left[\cos(1+\alpha_1)\theta + \frac{(3-\alpha_1)}{(1-\alpha_1)} \frac{\sin[\omega(1+\alpha_1)/2]}{\sin[\omega(1-\alpha_1)/2]} \cos(1-\alpha_1)\theta\right] / \sigma^I_{\theta\theta}(\theta=0) \\ \left[-\cos(1+\alpha_1)\theta + \frac{(1+\alpha_1)}{(1-\alpha_1)} \frac{\sin[\omega(1+\alpha_1)/2]}{\sin[\omega(1-\alpha_1)/2]} \cos(1-\alpha_1)\theta\right] / \sigma^I_{\theta\theta}(\theta=0) \\ \left[-\sin(1+\alpha_1)\theta + \frac{\sin[\omega(1+\alpha_1)/2]}{\sin[\omega(1-\alpha_1)/2]} \sin(1-\alpha_1)\theta\right] / \sigma^I_{\theta\theta}(\theta=0) \end{Bmatrix}$$

$$+A_2 r^{\alpha_2 - 1} \begin{Bmatrix} \left[\sin(1+\alpha_2)\theta + \frac{(3-\alpha_2)}{(1+\alpha_2)} \frac{\sin[\omega(1+\alpha_2)/2]}{\sin[\omega(1-\alpha_2)/2]} \sin(1-\alpha_2)\theta\right] / \sigma^{II}_{r\theta}(\theta=0) \\ \left[-\sin(1+\alpha_2)\theta + \frac{\sin[\omega(1+\alpha_2)/2]}{\sin[\omega(1-\alpha_2)/2]} \sin(1-\alpha_2)\theta\right] / \sigma^{II}_{r\theta}(\theta=0) \\ \left[\cos(1+\alpha_2)\theta - \frac{(1-\alpha_2)}{(1+\alpha_2)} \frac{\sin[\omega(1+\alpha_2)/2]}{\sin[\omega(1-\alpha_2)/2]} \cos(1-\alpha_2)\theta\right] / \sigma^{II}_{r\theta}(\theta=0) \end{Bmatrix} \tag{5}$$

In (3–5) we have used the following notations:

$$\sigma^I_{\theta\theta}(\theta=0) \stackrel{\text{def}}{=} \frac{(1+\alpha_1)}{(1-\alpha_1)} \frac{\sin[\omega(1+\alpha_1)/2]}{\sin[\omega(1-\alpha_1)/2]} - 1 \tag{6}$$

$$\sigma^{II}_{r\theta}(\theta=0) \stackrel{\text{def}}{=} 1 - \frac{(1-\alpha_2)}{(1+\alpha_2)} \frac{\sin[\omega(1+\alpha_2)/2]}{\sin[\omega(1-\alpha_2)/2]} \tag{7}$$

to normalize the "eigen-stresses" so that for mode I

$\sigma^{(1)}_{\theta\theta}(\theta=0) = 1$

and for mode II:

$\sigma^{(2)}_{r\theta}(\theta=0) = 1$

The solution (3)–(5) represents two in plane modes: Mode I which opens the V-notch faces and Mode II that shears the V-notch face along $x = 0$. A cracked or V-notched body may be subject to any of these modes or a combination, called "mixed mode" state.

To the best of our knowledge two failure criteria are available for V-notches under mixed mode loading Seweryn and Lukaszewicz (2002),Yosibash et al. (2006). In the next two subsections we provide a short overview of these criteria.

2.1 Seweryn criterion (Seweryn 1994; Seweryn and Lukaszewicz 2002)

The Seweryn criterion for mixed mode loading (Seweryn and Lukaszewicz 2002), which is a generalization of a mode I criterion presented by Novozhilov (1969) and validated by Seweryn (1994), postulates that failure initiates once the average circumferential stress along a precalculated damage length d_0 reaches a critical value (see Fig. 2):

$$R_f = \max_{\theta} \left[\frac{1}{d_0} \int_0^{d_0} \frac{\sigma_n(\theta)}{\sigma_c} dr\right] = 1 \tag{8}$$

where $\sigma_n(\theta)$ is the circumferential stress and σ_c is the material critical stress. The value of d_0 is calculated using the mode I criterion for a crack case (see Seweryn and Lukaszewicz (2002)):

$$d_0 = \frac{2K^2_{Ic}}{\pi \sigma^2_c} \tag{9}$$

where K_{Ic} denotes the fracture toughness. The criterion presented is applicable to brittle materials having high

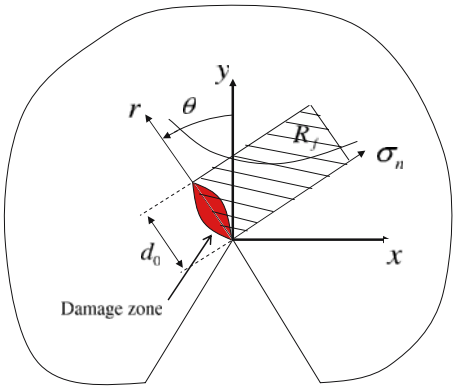

Fig. 2 Stress averaged over a length d_0 near the V-notch tip

critical shear stress τ_c. The Seweryn criterion takes a different form (incorporating τ_c dependency) for materials with low critical shear stresses.

The angle at which the maximum value of R_f is obtained is the crack initiation angle θ_f, and the load that induces $R_f = 1$ for the angle θ_f is the critical load.

2.2 Leguillon criterion (Yosibash et al. 2006)

Leguillon (2002) proposed a criterion for mode I failure initiation at a sharp V-notch tip based on a combination of the Griffith Energy Release Rate (ERR) criterion for a crack, and a strength criterion for a straight edge ($\omega = 180°$). This approach is based on the change in potential energy due to the creation of a small crack in the direction θ_0 which generates maximum change in potential energy. In Yosibash et al. (2006) the criterion was generalized to mixed mode loading. This criterion also makes use of a characteristic length ℓ_0, which is the distance from the V-notch tip at which both the ERR and strength criterion are met:

$$\ell_0 = \frac{G_c}{H_{11}(\omega,\theta_0) + m_\ell(\ell_0)(H_{12}(\omega,\theta_0) + H_{21}(\omega,\theta_0)) + m_\ell^2(\ell_0)H_{22}(\omega,\theta_0)} \left(\frac{\sigma_{\theta\theta}^{(1)}(\theta_0) + m_\ell(\ell_0)\sigma_{\theta\theta}^{(2)}(\theta_0)}{\sigma_c} \right)^2 \quad (10)$$

For a V-notch in an isotropic material under a state of mixed mode loading, the critical mode I GSIF A_{1c} is given by:

$$A_{1c} = \left(\frac{G_c}{H_{11}(\omega,\theta_0) + m_\ell(H_{12}(\omega,\theta_0) + H_{21}(\omega,\theta_0)) + m_\ell^2 H_{22}(\omega,\theta_0)} \right)^{\alpha_1 - 1} \left(\frac{\sigma_c}{\sigma_{\theta\theta}^{(1)}(\theta_0) + m_\ell \sigma_{\theta\theta}^{(2)}(\theta_0)} \right)^{2\alpha_1 - 1} \quad (11)$$

where G_c is the critical ERR and σ_c is the 1-D stress at brittle failure, both being material properties. The parameter m_ℓ is the mode mixity ratio and is taken as:

$$m_\ell = \frac{A_2}{A_1} \ell_0^{\alpha_1 - \alpha_2} \quad (12)$$

Notice that A_{1c} depends on θ_0 and the mode mixity ratio A_2/A_1. This means that for each θ_0 a different value of A_{1c} is obtained. Therefore, the angle θ_0 that produces the smallest value of A_{1c} for a given A_2/A_1 is the crack initiation angle, denoted by θ_f.

The $H_{ij}(\omega,\theta)$ functions depend on the local geometry and boundary conditions in the neighborhood of the V-notch tip and are computed by an integration procedure as shown in Yosibash et al. (2006). For example in Appendix A, the functions H_{ij} for different solid opening angles ω and material properties $E = 1\ MPa$, $\nu = 0.36$ are given (taken from Yosibash et al. (2006)). H_{ij} for any other elastic material can be computed by:

$$H_{ij}^{new}(\omega,\theta_0) = H_{ij}(\omega,\theta_0) \frac{1}{1-0.36^2} \frac{1-\nu^2}{E} \quad (13)$$

Correlation of this failure criterion with experimental observation in both PMMA and MACOR V-notched specimens under mixed mode loading shows good agreement (Yosibash et al. 2006).

It should be noted that the failure criteria in Yosibash et al. (2006) and the new failure criteria that will be presented in the sequel (GSED) are applicable to large mode mixity values $\frac{A_2}{A_1} \approx 10$ *but are not applicable to the pure mode II case where* $A_1 \to 0$

Leguillon's criterion provides better predictions compared to experimental observation than the Seweryn criterion (Yosibash et al. 2004) for mode I loading. Both the Seweryn criterion and the Leguillon criteria result in progressively worse predicted failure loads as the V-notch solid angle $\omega \to \pi$ because the GSIF for such large angles tends to a constant (large V-notch opening angles ($2\pi - \omega \geq 120^0$) are not often found in engineering practice).

More importantly the application of either the Leguillon or Seweryn failure criteria require many computations. We wish to propose herein a simpler failure criterion which is an extension of the SED failure criterion presented in Yosibash et al. (2004) for mode I loading.

3 Generalized strain energy density—A mixed mode failure initiation criterion

In this section, we generalize the failure criterion introduced in Lazzarin and Zmabardi (2001), Yosibash et al. (2004) named the strain energy density (SED) failure

criterion, to mixed mode loading at the V-notch tip. In the limit $\omega \to \pi$ and under uniform tension the SED criterion states that failure occurs once the SED in a circular region around the V-notch tip reaches a critical value SED_{cr} (Yosibash et al. 2004):

$$SED_{cr} = \frac{\sigma_c^2}{2E} \tag{14}$$

By requiring that the value of SED be equal at failure for the two extreme cases of the V-notch problem ($\omega = 2\pi$ and $\omega = \pi$) it was shown (Yosibash et al. 2004) that the material integration radius in which the SED should be computed is:

$$R_{mat}^{crack} = \frac{(1+\nu)(5-8\nu)K_{Ic}^2}{4\pi\sigma_c^2} \tag{15}$$

In (Yosibash et al. 2004) this integration radius was assumed to be independent of ω. In our generalization of the criterion we wish to elevate the constrain that R_{mat} is ω independent. We postulate that two criteria have to hold simultaneously at the instance of failure:

(1) The SED in a circular area Ω_R around the V-notch tip must exceed SED_{cr} (as in Yosibash et al. (2004)).
(2) The strain energy $\mathcal{U}$ in the same region Ω_R around the V-notch tip must exceed a critical material value $\mathcal{U}_{cr}$.

The value of $\mathcal{U}_{cr}$ can be calculated from the crack case by:

$$\begin{aligned}\mathcal{U}_{cr} = SED_{cr} \times \Omega_R = SED_{cr} \times b\pi \left(R_{mat}^{crack}\right)^2 \\ = \frac{b(1+\nu)^2(5-8\nu)^2}{32\pi E}\frac{K_{Ic}^4}{\sigma_c^2}\end{aligned} \tag{16}$$

where b is the width of the structure.

For a general stress state under the assumption of plane strain the expression for the strain energy is:

$$\begin{aligned}\mathcal{U}(\boldsymbol{u})[R] = \frac{b}{2}\iint_{\Omega_R}\sigma_{jk}\epsilon_{jk}d\Omega = \frac{(1+\nu)b}{2E} \\ \times \iint_{\Omega_R}\Big[(1+\nu)(\sigma_{rr}^2+\sigma_{\theta\theta}^2) \\ -2\nu\sigma_{rr}\sigma_{\theta\theta}+2\sigma_{r\theta}^2\Big]d\Omega\end{aligned} \tag{17}$$

Inserting (5) in (17):

$$\begin{aligned}\mathcal{U}(\boldsymbol{u})[R] = \frac{b(1+\nu)A_1^2R^{2\alpha_1}}{2E}\int_{\frac{\omega-\pi}{2}}^{\frac{\omega+\pi}{2}}\Bigg(\frac{F_{11}(\theta,\omega)}{2\alpha_1} \\ + 2m_R\frac{F_{12}(\theta,\omega)}{\alpha_1+\alpha_2} + m_R^2\frac{F_{22}(\theta,\omega)}{2\alpha_2}\Bigg)d\theta\end{aligned} \tag{18}$$

where $m_R = \frac{A_2}{A_1}R^{\alpha_2-\alpha_1}$ and $F_{ij}(\omega,\theta)$ are given by :

$$\begin{aligned}F_{11} = (1-\nu)\left[\left(\sigma_{rr}^{(1)}(\theta,\omega)\right)^2 + \left(\sigma_{\theta\theta}^{(1)}(\theta,\omega)\right)^2\right] \\ -2\nu\sigma_{rr}^{(1)}(\theta,\omega)\sigma_{\theta\theta}^{(1)}(\theta,\omega) + 2\left(\sigma_{r\theta}^{(1)}(\theta,\omega)\right)^2\end{aligned}$$

$$\begin{aligned}F_{12} = (1-\nu)\left(\sigma_{rr}^{(1)}(\theta,\omega)\sigma_{rr}^{(2)}(\theta,\omega)\right. \\ \left.+\sigma_{\theta\theta}^{(1)}(\theta,\omega)\sigma_{\theta\theta}^{(2)}(\theta,\omega)\right) \\ -\nu\left(\sigma_{\theta\theta}^{(1)}(\theta,\omega)\sigma_{rr}^{(2)}(\theta,\omega)\right. \\ \left.+\sigma_{\theta\theta}^{(2)}(\theta,\omega)\sigma_{rr}^{(1)}(\theta,\omega)\right) \\ +2\sigma_{r\theta}^{(1)}(\theta,\omega)\sigma_{r\theta}^{(2)}(\theta,\omega)\end{aligned} \tag{19}$$

$$\begin{aligned}F_{22} = (1-\nu)\left[\left(\sigma_{rr}^{(2)}(\theta,\omega)\right)^2 + \left(\sigma_{\theta\theta}^{(2)}(\theta,\omega)\right)^2\right] \\ -2\nu\sigma_{rr}^{(2)}(\theta,\omega)\sigma_{\theta\theta}^{(2)}(\theta,\omega) + 2\left(\sigma_{r\theta}^{(2)}(\theta,\omega)\right)^2\end{aligned} \tag{20}$$

Because both the SED and $\mathcal{U}$ are to be equal to SED_{cr} and $\mathcal{U}_{cr}$ simultaneously at the instance of failure, from (16) and (14) one obtains:

$$\begin{aligned}\mathcal{U}_{cr} = SED_{cr}\frac{\omega}{2\pi}\pi\left(R_{mat}^{notch}\right)^2 b \\ \Downarrow \\ R_{mat}^{notch} = \frac{(1+\nu)(5-8\nu)}{\sqrt{8\pi\omega}}\left(\frac{K_{Ic}}{\sigma_c}\right)^2\end{aligned} \tag{21}$$

R_{mat}^{notch} is a function of the V-notch angle and the material constants. For the case of $\omega = 2\pi$ we obtain $R_{mat}^{notch} = R_{mat}^{crack}$.

Consider for example a specimen made of PMMA or MACOR with the following material elastic parameters: $E = 3100\,MPa$, $\nu = 0.36$, $\sigma_c = 112\,MPa$, $K_{Ic} = 1.12\,MPa\sqrt{m}$, and correspondingly $E = 66900\,MPa$, $\nu = 0.3$, $\sigma_c = 103\,MPa$, $K_{Ic} = 1.2\,MPa\sqrt{m}$. In Table 1 $R_{mat}^{notch}(\omega)$ as $\omega \to \pi$ is provided.

Remark 1 *The assumption in Yosibash et al. (2004) that the integration radius R_{mat} is independent of ω may have been one of the reasons that the original SED criterion yielded only a low estimate to the failure load.*

By equating (18) and (16) and inserting the value of R_{mat}^{notch} one can obtain an expression for the generalized stress intensity factor (GSIF) at failure:

Table 1 R_{mat}^{notch} [mm] for different V-notch solid angle ω, for PMMA and MACOR

ω	360	345	330	315	300	285	270	255	240
PMMA (mm)	0.0229	0.0234	0.0239	0.0245	0.0251	0.0257	0.0264	0.0272	0.0281
MACOR (mm)	0.0373	0.0381	0.0390	0.0399	0.0409	0.0419	0.0432	0.0444	0.0458

Table 2 PMMA material properties

T [K]	σ_c [MPa]			E [MPa]	ν	K_{IC} $MPa\sqrt{m}$				
	Test 1	Test 2	Avg			Test 1	Test 2	Test 3	Test 4	Avg
296	105.8	117.8	111.8	3,100	0.36	1.03	1.07	1.15	1.25	1.12
233	158	168	163	4,300	0.36	1.75	1.98	–	–	1.86
200	173	186	179.5	4,980	0.36	2.0881	2.253	–	–	2.17

$$A_{1c} = \sqrt{\frac{K_{Ic}^4(5-8\nu)^2(1+\nu)}{16\pi\sigma_c^2\left(R_{mat}^{notch}\right)^{2\alpha_1}}\left(\int_{-\frac{\omega}{2}}^{\frac{\omega}{2}}\left(\frac{F_{11}(\theta,\omega)}{2\alpha_1}+2m_R\frac{F_{12}(\theta,\omega)}{\alpha_1+\alpha_2}+m_R^2\frac{F_{22}(\theta,\omega)}{2\alpha_2}\right)\right)^{-1}} \quad (23)$$

Notice that A_{1c} is a function of the material properties and mixity ratio but not of A_1. For a given V-notch geometry and loading configuration one can predict the critical load for failure by calculating the value of A_1 for a unit load and the value of A_{1c} by (23). Since the material is considered elastic one can easily compute the critical load:

$$P_{cr} = \frac{A_{1c}}{A_1} \quad (24)$$

One can also use the value of the SED, in a circular sector around the V-notch tip defined by R_{mat}^{notch}, directly for obtaining the critical load.

$$P_{cr} = \sqrt{\frac{SED_{cr}}{SED}} \quad (25)$$

To distinguish between the current failure criterion and that of Yosibash et al. (2004) we denote the present one by Generalized Strain Energy Density (GSED). In the limit $\omega \to 2\pi$, the GSED criterion should predict failure initiation for the mixed mode crack case. This topic is addressed in Appendix B.

4 Experiments on failure initiation at V-notch tips under mixed mode loading

To validate the failure criteria, we conducted several mixed mode experiments on PMMA and MACOR (machinable glass ceramics by Aremco Products, Inc) V-notched bar specimens. In this section we describe the experimental procedures and provide mechanical properties of tested materials.

4.1 Experiments on PMMA

The first set of experiments was performed on V-notched PMMA bar specimens $80 \times 10 \times 10$ and $80 \times 10 \times 15$ (mm) containing a V-notch with a solid angle of $\omega = 315°$. The V-notch tip radius was $\rho = 0.03\,mm$. The value of the PMMA elastic constants and fracture toughness were experimentally obtained for different test temperatures as summarized in Table 2. The specimens were loaded in a non symmetric Three Point Bending 3PB configuration in order to obtain a state of mixed mode at the V-notch tip (see Fig. 3).

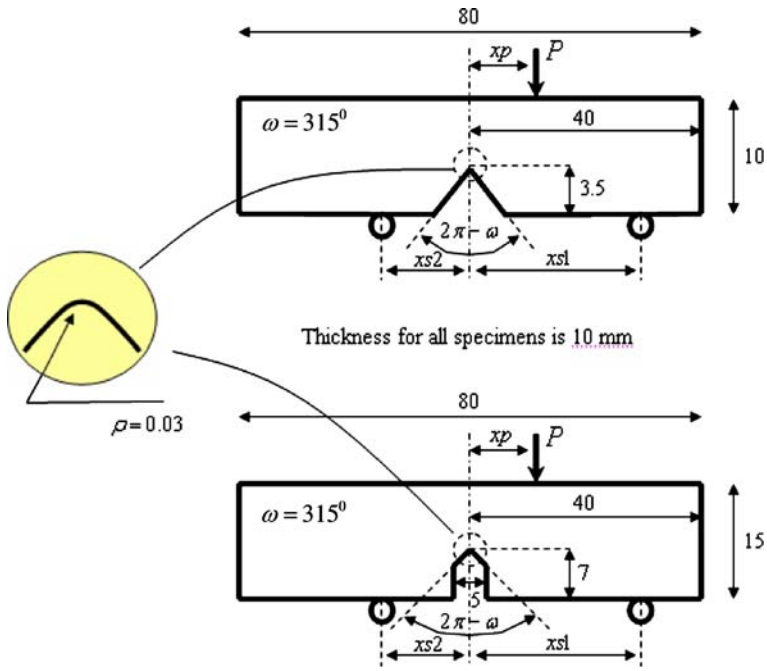

Fig. 3 PMMA specimens: dimensions and loading configuration

Remark 2 Finite element analysis prior to the experimental procedure suggested a Four Point Bending (4PB) configuration to yield a wider range of mode mixity ratios. However, preliminary experiments under 4PB on PMMA specimens resulted in large bending without breaking so 3PB configuration was adopted instead.

The PMMA samples were divided into 5 sets (a,b1, b2,c,d) varying in geometric dimensions and test temperatures. All sets had a notch radius of $\rho = 0.03\ mm$ except set b1 for which $\rho = 0.25\ mm$. The dimensions, material properties, failure loads and crack initiation angles are summarized in Table 3. Figure 4 presents a closeup at the V-notch tips after fracture and the crack initiation angles. In all test cases the failure initiated at the notch tip and propagated towards the point at which the load is applied (see Fig. 5). We excluded sets a,b1 and c from subsequent analysis because specimens a and c are loaded by mode I only and set b1 contained a large notch tip radius whereas the failure criterion is for sharp V-notches. Their experimental results are provided for completeness only.

4.2 Experiments on MACOR

A plate of MACOR (Machinable Glass Ceramic by Aremco Products, Inc) was cut into 50 80x18x10 mm bars. In these bars we inserted a V-notch with an opening angle of 45 degrees, notch depth of 7 mm and a notch tip radius of $\rho = 0.03$ mm (see Fig. 6). The following material properties were reported by Aremco $E = 66900\ MPa$, $\sigma_c = 103\ MPa$, $\nu = 0.3$ and $K_{IC} = 1.53\ MPa\sqrt{m}$. Ultrasonic inspection of the material and a flexural test conducted on one bar specimen confirm the value of E and σ_c reported. The value of the fracture toughness as reported by Aremco does not agree with our estimation to be between 1.1 and 1.2 $MPa\sqrt{m}$ (the fracture toughness reported by Aremco is a generic value and not obtained from tests on the batch from which the specimens where manufactured).

The MACOR samples were loaded by 4PB because a wider range of A_2/A_1 ratios can be obtained compared to 3PB loading. As in the case of PMMA specimens, post-experiment examination showed that failure initiated from the notch tip and propagated in the direction of the applied load. The dimensions, failure loads and crack initiation angles are summarized in Table 4 (Fig. 7).

5 Validation of the failure criteria

To check the validity of the various failure criteria we performed finite element analysis on models represent-

Table 3 Dimensions, material properties and experimental results for PMMA specimens

Specimen	E	Configuration [mm]			L/H/b [mm]	T	Failure load	Crack initiation angle
#	[MPa]	$xp1$	$xs1$	$xs2$	b = thickness	[K]	[N]	[deg]
a-1	3,100	0	20	20	$55 \times 10 \times 10$	296	278	90
b1-1	3,100	0	20	20	$80 \times 10 \times 10$	296	294	90
b1-2	3,100	2	18	22	$80 \times 10 \times 10$	296	317	85
b1-3	3,100	6	14	26	$80 \times 10 \times 10$	296	327	80
b1-4	3,100	10	10	30	$80 \times 10 \times 10$	296	533	68
b1-5	3,100	13.5	6.5	33.5	$80 \times 10 \times 10$	296	744	60
b1-6	3,100	16	4	36	$80 \times 10 \times 10$	296	1,280	50
b2-1	3,100	0	20	20	$80 \times 10 \times 10$	296	173	90
b2-2	3,100	2	18	22	$80 \times 10 \times 10$	296	226	85
b2-3	3,100	6	14	26	$80 \times 10 \times 10$	296	301	79
b2-4	3,100	10	10	30	$80 \times 10 \times 10$	296	408	72
b2-5	3,100	13.5	6.5	33.5	$80 \times 10 \times 10$	296	613	68
b2-6	3,100	16	4	36	$80 \times 10 \times 10$	296	998	60
c	3,100	0	20	20	$80 \times 15 \times 10$	296	270	90
d-1	4,980	0	20	20	$80 \times 15 \times 10$	198	470	90
d-2	4,980	3	17	23	$80 \times 15 \times 10$	198	510	85
d-3	4,980	6	14	26	$80 \times 15 \times 10$	198	570	78
d-4	4,980	10	10	30	$80 \times 15 \times 10$	198	760	75
d-5	4,980	14.5	5.5	34.5	$80 \times 15 \times 10$	198	1,200	60
d-6	4,980	15.5	4.5	35.5	$80 \times 15 \times 10$	198	1,410	54
d-7	4,980	17	3	37	$80 \times 15 \times 10$	198	1,660	**

**Crack initiation angle for d-7 specimen could have not been determined due to massive fracture damage in the V-notch vicinity

ing the experimental specimens to extract the required parameters used by the failure criteria. p-Version FE 2-D (Szabó and Babuška 1991) models representing the experimental specimens were generated and solved.

In the experiments a 3-D stress state exists which can be accurately represented by a 2-D plane strain model. This assumption was verified by comparing between the stress state of a 3-D and 2-D FE model. Note in Fig. 8 that at a distance of $0.02\,mm$ from the free edge the stress state is constant with respect to the z-axis, similar to the 2-D plane strain situation.

In order to minimize the idealization error, caused by the unknown force distribution induced by the loading process, we conducted sensitivity tests. The area of applied load and supports was changed $(0.1-1\,mm)$ in order to verify that it has no effect on data extracted at the V-notch tip. In order to minimize the discretization error a graded mesh of elements was created around the V-notch tip singularity and the load and support areas (see Fig. 9).

All FE models used for extracting the various ingredients needed for the failure criteria had an error in energy norm which did not exceed 1.5%.

5.1 Predicted vs. experimental failure load in PMMA specimens

To check the validity of the Leguillon and GSED failure criteria we extracted the value of the GSIFs and associated eigen-pairs for a unit load from the FE-models and computed the value of the GSIF at failure. In order to apply the Seweryn failure criterion, we computed the value of the failure function R_f for the failure load in the precalculated damage zone (according to the criterion the value of R_f at failure should equal 1). In

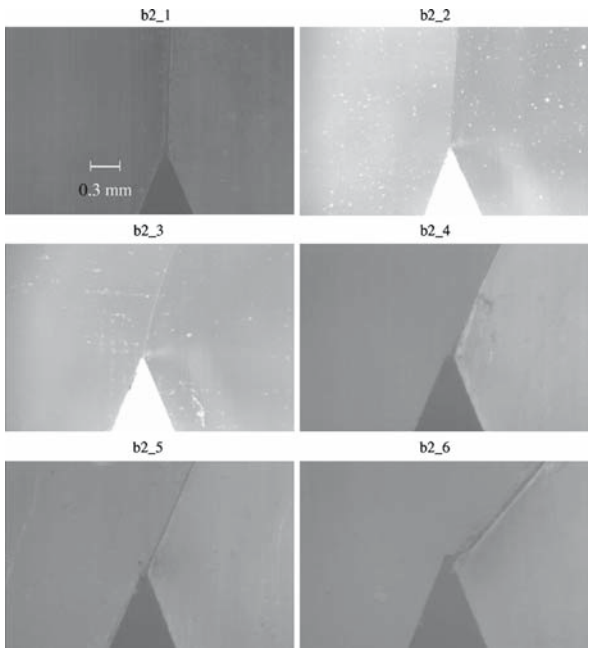

Fig. 4 Crack initiation at several PMMA samples tested at 296 K—Closeup photos at tip

Appendix A all calculated and extracted values used to predict failure initiation are shown. Table 5 and Fig. 10 summarize all experimental and prediction results for our PMMA tests for the various load mixity ratios.

As a result of the lower and upper bounds for the PMMA fracture toughness lower and upper bounds to the failure load is predicted. The crack initiation angle prediction does not seem to be effected by variations in the fracture toughness used.

For PMMA experiments conducted at room temperature (set b2) the GSED and Leguillon failure criteria predict the failure load well. The Seweryn criterion under-predicts the failure load in all cases and the predicted value deteriorates as the mode mixity ratio increases. The crack initiation angle is well predicted by both the Seweryn and Leguillon criteria. For the experimental set d all three criteria predict well the failure load. The crack initiation angle is predicted well by Leguillon's criterion but Seweryn's criterion over-predicts the crack initiation angle as the mode mixity ratio increases.

5.2 Predicted vs. experimental failure load in MACOR specimens

The validity of the various failure criteria was also checked for the MACOR experiments. Table 6 and Fig. 11 summarize experimental and predicted failure load and failure angle for MACOR specimens. All criteria applied predict well the failure load and crack initiation angle but the scatter of experimental results especially for mode mixity values of $\frac{A_2}{A_1}^{\alpha_1-\alpha_2} > 2$ makes it difficult to determine which criterion predicts better the failure initiation. If one takes into account the average value of experimental points for each mode mixity ratio then the GSED criterion predicts the failure load more accurately and the Leguillon criterion is better for the crack initiation angle.

Fig. 5 PMMA specimens after failure: set *d c* and *a*

5.3 Analysis of experimental data reported by Seweryn and Lukaszewicz (2002)

Seweryn and Lukaszewicz (2002) conducted experiments on PMMA double V-notched plates (see Fig. 12) using a device which is reported to induce mode mixity at the notch tip *for different V-notch solid angles* ω. FE models simulating the specimens and loading condition were verified by comparing our extracted GSIF to the values reported in Seweryn and Lukaszewicz (2002). Similarly to the analysis described in the previous subsections GSIF were extracted for a unit load applied and compared to the calculated critical GSIF for both the Leguillon and GSED criteria. In order to predict failure load for the Seweryn criterion the value of R_f for the failure load along d_0, was calculated. Table 7 and Fig. 13 summarize experimental results in Seweryn and Lukaszewicz (2002) for a variety of V-notch solid angles ω and mode mixity ratios, and our predicted values. In general all failure criteria predict well the failure load. For $\omega = 300°, 280°$ when the mode mixity ratio is larger than $\frac{A_2}{A_1}^{\alpha_1-\alpha_2} \approx 1.5\, mm^{-0.134}$ the Leguillon and Seweryn criteria over-predict the failure load. The crack initiation angle is predicted well for all but $\omega = 280°$ set where for all mode mixity values both the Leguillon and Seweryn criteria over-predict the crack initiation angle.

6 Conclusions

The goal of our work was to verify the predicted failure load and failure initiation angle by three mixed mode failure criteria for brittle elastic V-notched structures. Two are documented in Seweryn and Lukaszewicz (2002), Yosibash et al. (2006) and a third new criterion, the GSED criterion, is an extension of a known mode I failure criterion in Yosibash et al. (2004). The validity of the three failure criteria for predicting failure initiation at *sharp* V-notch tips under mixed mode loading has been examined and compared to experimental results. The experiments included: loading of specimens made of two different elastic materials (PMMA and MACOR) under three and four point bending conditions which induce a state of mixed mode at the V-notch tip. Mixed mode experimental results reported in Seweryn and Lukaszewicz (2002) for PMMA specimens with a large range of V-notch solid angles ω and mode mixity values have also been examined. All cri-

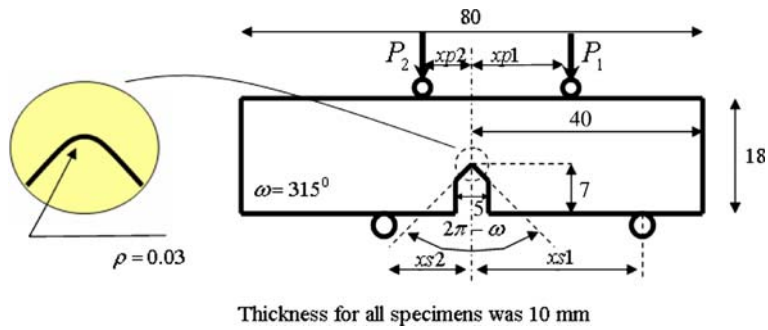

Fig. 6 MACOR specimens dimensions and loading configuration

Table 4 Dimensions and experimental results for MACOR specimens

Specimen #	Configuration [mm]				L/H/b [mm]	T [K]	Failure load [N]	Crack initiation angle [deg]
	$xp1$	$xp2$	$xs1$	$xs2$				
M-6	30	0	20	30	80 × 18 × 10	296	2,200	70
M-7	30	10	20	30	80 × 18 × 10	296	2,800	46
M-8	30	13	20	30	80 × 18 × 10	296	3,370	43
M-9	30	15	20	30	80 × 18 × 10	296	5,540	33
M-10	30	17	20	30	80 × 18 × 10	296	6,590	27
M-11	30	17	20	30	80 × 18 × 10	296	4,720	45
M-12	30	15	20	30	80 × 18 × 10	296	3,980	55
M-13	30	13	20	30	80 × 18 × 10	296	3,300	58
M-14	30	10	20	30	80 × 18 × 10	296	2,160	46
M-20	30	17	20	30	80 × 18 × 10	296	5,740	30
M-21	30	15	20	30	80 × 18 × 10	296	4,130	52
M-22	30	13	20	30	80 × 18 × 10	296	2,760	40
M-23	30	10	20	30	80 × 18 × 10	296	2,730	65

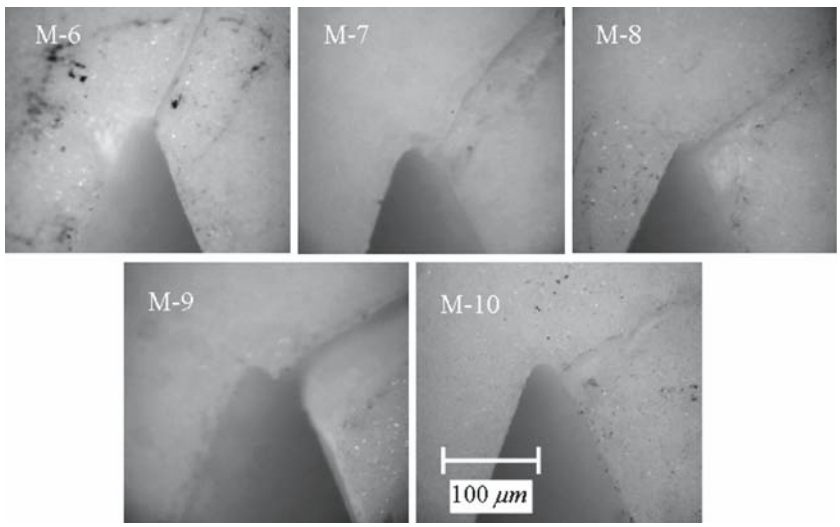

Fig. 7 V-notch area of some of the MACOR samples after failure

teria seem to predict both the failure load and crack initiation angle with a 80–100% accuracy. For failure load prediction there is no definite "best criterion" but the GSED is easier to apply requiring only the calculation of the material notch integration radius and the calculation of SED or the resulting A_{1c}. The crack initiation angle is best predicted by using the Leguillon criterion.

The failure criteria validated herein assume a sharp V-notch tip whereas the experimental specimens contain a small V-notch tip radius ρ (see Fig. 3). In future work a correction to the mixed mode failure criteria accounting for ρ will be developed.

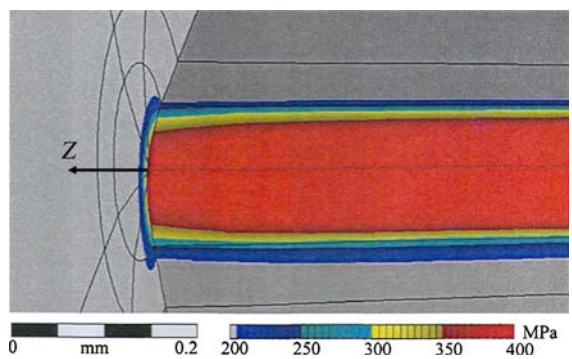

Fig. 8 Stress state in the V-notch vicinity for a 3-D V-notched bar under mixed mode loading

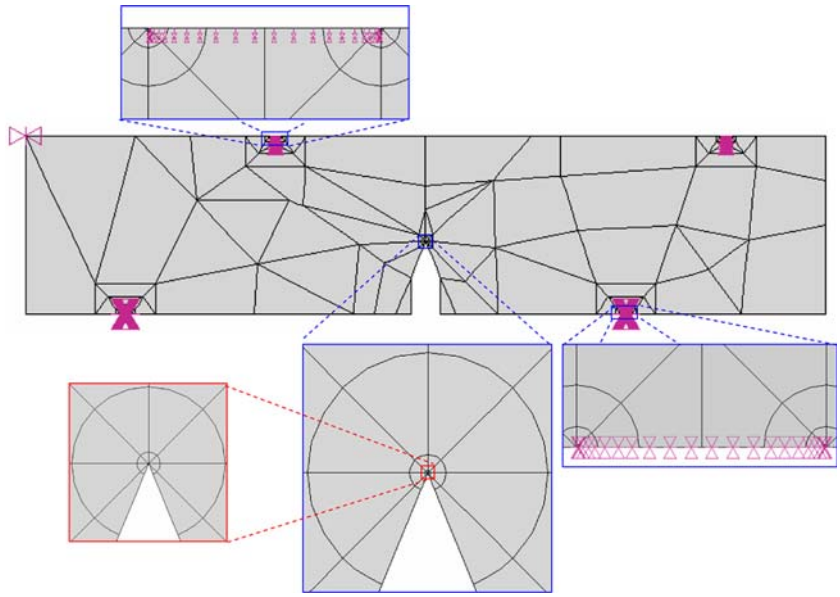

Fig. 9 Typical p-FE model, graded mesh around V-notch tip, load and support areas

Table 5 Experimental and predicted failure load and crack initiation angle in PMMA specimens

Set	$\frac{A_2}{A_1}^{\alpha_1-\alpha_2}$	Experiments		Seweryn (N,deg)			Leguillon (N,deg)			GSED (N)	
	$[mm^{-0.154}]$	Failure load N	Crack initiation angle	Low	High	Angle	Low	High	Angle	Low	High
b2-2	0.07	226	85°	124	147	85	165	200	86	161	195
b2-3	0.156	301	79°	157	186	80	208	252	82	204	246
b2-4	0.217	408	72°	226	267	76	297	359	77	289	349
b2-5	0.333	613	68°	351	414	70	462	536	73	448	541
b2-6	0.616	998	60°	576	678	67	748	898	63	718	860
d-2	0.110	510	85°	341	364	85	465	501	83	449	480
d-3	0.190	570	77°	405	433	80	551	594	80	532	568
d-4	0.290	760	75°	567	605	76	766	825	75	739	789
d-5	0.530	1,200	60°	1,006	1,073	70	1,336	1,436	63	1,289	1,374
d-6	0.686	1,410	54°	1,200	1,279	67	1,579	1,694	60	1,513	1,611

Table 6 Experimental and predicted failure load and crack initiation angle in MACOR specimens

Specimen	$\frac{A_2}{A_1}^{\alpha_1-\alpha_2}$	Experiments				Seweryn [N]			Leguillon [N]			GSED [N]	
	$[mm^{-0.154}]$	Failure load [N]			Avg - angle [deg]	Low	High	Angle	Low	High	Angle	Low	High
M-6	0.342	2,200	–	–	70	1,579	1,702	77	2,102	2,286	73	2,040	2,220
M-7,14,23	1.308	2,160	2,730	2,800	46	2,409	2,580	50	3,029	3,267	50	2,751	2,957
M-8,13,22	1.737	2,760	3,300	3,370	48	3,070	3,306	43	3,845	4,138	45	3,463	3,710
M-9,12,21	2.200	3,980	4,130	5,540	46	3,806	4,065	40	4,710	4,086	40	4,366	5,058
M-10,11,20	3.250	4,700	5,740	6,590	34	4,860	5,280	39	5,886	6,300	35	4,784	5,095

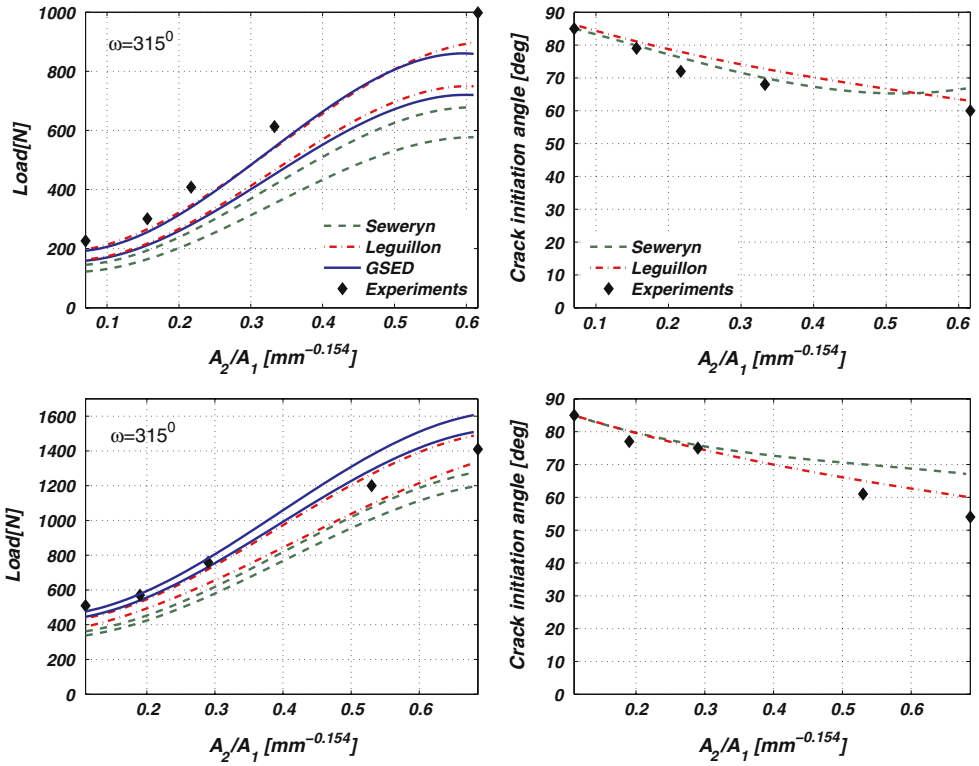

Fig. 10 Experiments and predicted failure load and crack initiation angle for PMMA sets: **b2 (296 K)**-top **d (200 K)**-bottom

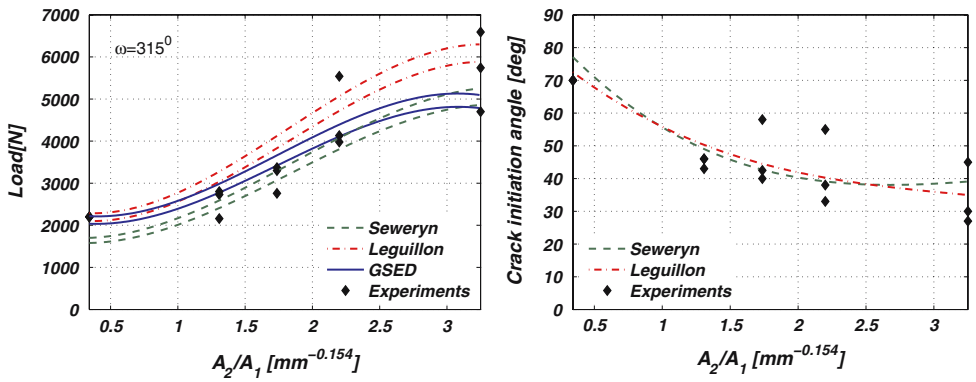

Fig. 11 Experiments and predicted failure load and crack initiation angle for MACOR specimens

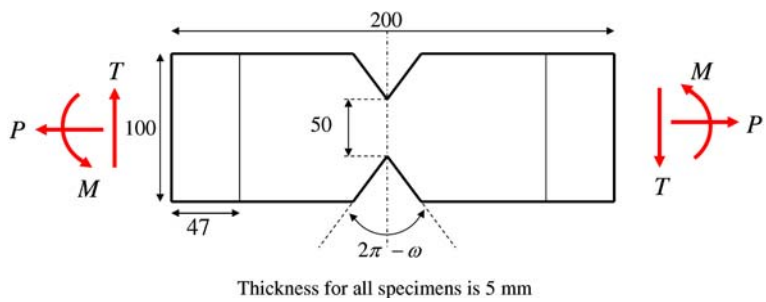

Fig. 12 PMMA specimens reported in Seweryn and Lukaszewicz (2002): Dimensions and loading configuration

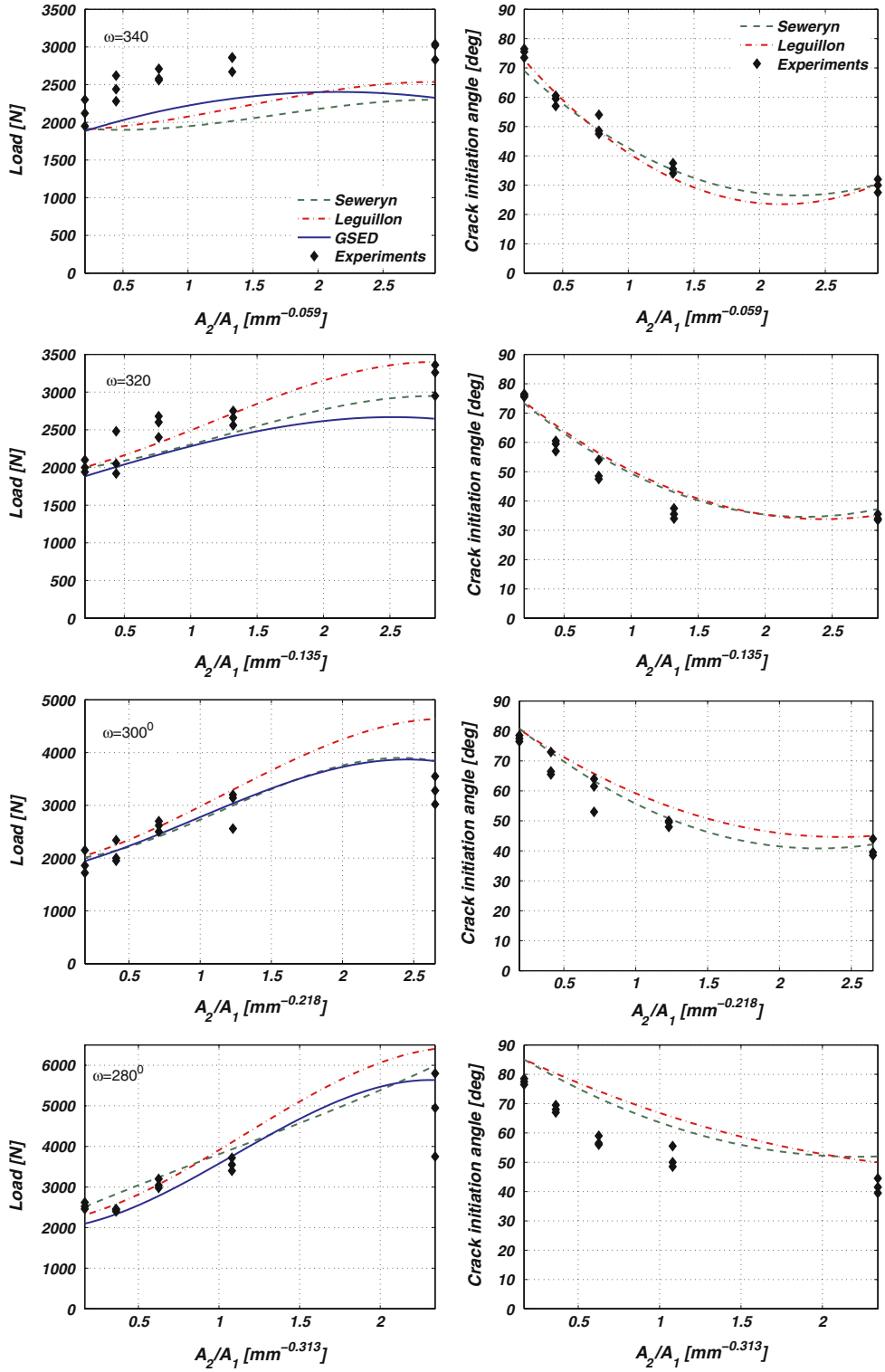

Fig. 13 Experiments and predicted failure load and crack initiation angle for PMMA experiments in Seweryn and Lukaszewicz (2002)

Table 7 Predicted failure load and failure angle compared to experiments reported in Seweryn and Lukaszewicz (2002)

ω	A_2/A_1 $[mm^{\alpha_1-\alpha_2}]$	Average experimental values (Seweryn and Lukaszewicz 2002)		Seweryn		Leguillon		GSED
		θ_c [deg]	Avg. Failure load [N]	θ_c [deg]	Failure load [N]	θ_c [deg]	Failure load [N]	Failure load [N]
340	0.207	75	2,120	72	1,918	75	1,906	1,811
	0.447	59	2,450	57	1,900	60	1,936	2,076
	0.776	46	2,620	46	1,918	45	2,014	2,198
	1.343	36	2,780	38	2,016	35	2,184	2,252
	2.895	30	3,010	30	2,300	30	2,535	2,333
320	0.213	75	2,013	75	2,004	75	2,008	1,887
	0.460	65	2,150	64	2,044	65	2,118	1,997
	0.797	52	2,560	53	2,211	55	2,334	2,177
	1.381	48	2,656	45	2,456	45	2,717	2,413
	2.975	35	3,190	37	2,948	35	3,399	2,646
300	0.190	78	1,910	82	2,022	80	2,050	1,950
	0.410	68	2,010	72	2,123	75	2,237	2,127
	0.710	60	2,610	62	2,426	65	2,605	2,462
	1.231	49	2,970	52	2,993	55	3,295	3,033
	2.652	41	3,280	42	3,842	45	4,637	3,838
280	0.172	75	2,533	85	2,528	85	2,320	2,102
	0.371	65	2,480	79	2,789	80	2,565	2,324
	0.643	55	3,070	72	3,269	75	3,075	2,787
	1.113	50	3,556	62	3,922	65	4,101	3,756
	2.400	40	4,833	52	5,992	50	6,404	5,636

Acknowledgements The authors thank Mr. Moshe Kupiec for his help in performing the experiments. This research has been partially funded by the VATAT-VEE grant number 86/06.

Appendix

A. All values used for predicting failure initiation

Here we include all extracted and calculated values used for predicting failure initiation by the different criteria (Tables 8–12).

Units for all tables are: $MPa\ m^{\alpha_1-1}$ for the GSIF, $\frac{N}{mm^2}$ for the SED, mm for all lengths.

B. GSED criterion for crack under mixed mode loading

In the limit when $\omega = 2\pi$ the V-notch becomes a crack. When only mode I is considered the GSED criterion reduces to the classical Irwin type failure criterion in which failure occurs if $K_I \geq \sqrt{2\pi} A_{1c}$. When mixed mode is considered it can be shown that the criterion predicts a failure envelope which can be expressed as:

$$\left(\frac{K_I}{K_{Ic}}\right)^2 + \left(\frac{K_I}{\alpha K_{Ic}}\right)^2 = 1 \tag{26}$$

This form of failure envelope is known as the empirical elliptical failure criterion Chang et al. (2006) where α is the relation between the mode I and mode II fracture toughness value. In order to determine the value of α for the GSED criterion one needs to determine what is the value of K_{II} at failure for the case of pure shear. Since the GSED criterion, in its current form, is not applicable to the case of pure mode II loading we used the predicted value of K_{II} at failure for very high mode mixity ratios $\frac{A_2}{A_1} \approx 10$. The value of $K_{II}^{failure}$ was calculated by $K_{II}^{failure} = \sqrt{2\pi} \cdot \frac{A_2}{A_1} \cdot A_{1c}$. We then defined α to be $\alpha = \frac{K_{II}^{failure}}{K_{Ic}}$.

Table 8 H_{ij} for $\omega = 315°, 330°, 300°$ $(E = 1\,MPa, \nu = 0.36)$ from Yosibash et al. (2006)

θ_0	$\omega = 330°$			$\omega = 315°$			$\omega = 300°$		
	H_{11}	H_{22}	$H_{12}+H_{21}$	H_{11}	H_{22}	$H_{12}+H_{21}$	H_{11}	H_{22}	$H_{12}+H_{21}$
30°	3.0965	5.5913	6.3403	3.0600	4.6212	5.8688	2.9552	3.8332	5.4388
35°	3.3952	5.4651	6.2988	3.3566	4.5299	5.8488	3.2627	3.7196	5.3466
40°	3.6885	5.3045	6.1559	3.6476	4.4054	5.7318	3.5502	3.6272	5.2614
45°	3.9718	5.1185	5.9101	3.9283	4.2551	5.5158	3.8272	3.5085	5.0809
50°	4.2404	4.9168	5.5623	4.1941	4.0878	5.2013	4.0893	3.3713	4.8056
55°	4.4899	4.7095	5.1159	4.4204	3.9126	4.7917	4.3320	3.2242	4.4384
60°	4.7160	4.5062	4.5770	4.6634	3.7380	4.2840	4.5515	3.0756	3.9847
65°	4.9146	4.3163	3.9539	4.8591	3.5741	3.7161	4.7439	2.9337	3.4519
70°	5.0822	4.1482	3.2571	5.0243	3.4282	3.0544	4.9061	2.8061	2.8499
75°	5.2159	4.0094	2.4988	5.1552	3.3076	2.3443	5.0352	2.6994	2.1902
80°	5.3132	3.9058	1.6930	5.2510	3.2161	1.5881	5.1291	2.6192	1.4858
85°	5.3722	3.8418	0.8550	5.3096	3.1502	0.8003	5.1860	2.5694	0.7509
90°	5.3920	3.8202	5.614E−04	5.3287	3.1409	6.753E−04	5.2051	2.5525	7.06E−04

Table 9 H_{ij} for $\omega = 270°, 240°$ $(E = 1, \nu = 0.36)$ from Yosibash et al. (2006)

θ_0	$\omega = 270°$			$\omega = 240°$		
	H_{11}	H_{22}	$H_{12}+H_{21}$	H_{11}	H_{22}	$H_{12}+H_{21}$
30°	2.5878	2.4714	4.1873	1.9182	1.4851	2.8891
35°	2.8676	2.4660	4.2622	2.1729	1.5340	3.0419
40°	3.1422	2.4273	4.2538	2.4258	1.5576	3.1330
45°	3.4071	2.3605	4.1586	2.6672	1.5339	3.1272
50°	3.6578	2.2721	3.9755	2.8974	1.4858	3.0418
55°	3.8903	2.1691	3.7059	3.1120	1.4193	2.8760
60°	4.1005	2.0594	3.3540	3.3069	1.3412	2.6319
65°	4.2848	1.9504	2.9264	3.4786	1.2590	2.3144
70°	4.4346	1.8601	2.4001	3.6194	1.1764	1.9522
75°	4.5492	1.7913	1.7977	3.7232	1.0988	1.5743
80°	4.6220	1.7565	1.2856	3.7979	1.0401	1.1447
85°	4.6633	1.7540	0.6647	3.8419	1.0041	0.6809
90°	4.6793	1.7506	3.266E−3	3.8536	0.9875	6.23E − 3

In classical fracture mechanics α is obtained by applying the maximum circumferential stress criterion Anderson (2005) to the case of pure mode II shear loading resulting in $\alpha = \frac{K_{IIc}}{K_{Ic}} = 0.866$.

There are many experiments that show that for brittle materials α is within 10% of this theoretical value. Table 13 shows different experimental values for α reported in literature and the values calculated by the GSED criterion.

Clearly the results for α as calculated by the GSED criterion are 33% lower then the theoretical value of $\alpha = 0.866$ and 25% lower then the lowest known experimental result. Future work is aimed at investigating this discrepancy.

Table 10 Calculated data for PMMA experiments

Specimen #	Seweryn				Leguillon			GSED						SED_{cr}
								Low			High			
	d_o^{low}	d_o^{high}	R_f^{low}	R_f^{high}	A_1	A_{1c}^{low}	A_{1c}^{high}	R_{mat}^{notch}	A_{1c}^{low}	SED_{low}^f	R_{mat}^{notch}	A_{1c}^{high}	SED_{high}^f	
$b2-2$	0.054	0.079	1.81	1.53	18.16	13.33	16.07	0.0208	12.94	3.97	0.030	15.67	2.70	2.016
$b2-3$	0.054	0.079	1.91	1.61	19.04	13.22	16	0.0208	12.87	4.41	0.030	15.58	3.01	2.016
$b2-4$	0.054	0.079	1.80	1.53	18.04	13.13	15.87	0.0208	12.79	4.01	0.030	15.47	2.74	2.016
$b2-5$	0.054	0.079	1.74	1.48	17.18	12.97	15.05	0.0208	12.57	3.76	0.030	15.17	2.58	2.016
$b2-6$	0.054	0.079	1.73	1.47	16.09	12.07	14.49	0.0208	11.58	3.89	0.030	13.86	2.71	2.016
$d-2$	0.086	0.1	1.49	1.39	29.67	22.85	25.67	0.033	26.11	4.17	0.038	27.93	3.64	3.23
$d-3$	0.086	0.1	1.40	1.31	27.78	22.68	25.46	0.033	25.91	3.71	0.038	27.70	3.25	3.23
$d-4$	0.086	0.1	1.34	1.25	26.25	22.36	25.08	0.033	25.52	3.41	0.038	27.27	3.00	3.23
$d-5$	0.086	0.1	1.19	1.11	22.43	21.15	23.64	0.033	24.09	2.80	0.038	25.69	2.46	3.23
$d-6$	0.086	0.1	1.17	1.10	21.50	20.40	22.76	0.033	23.08	2.80	0.038	24.57	2.47	3.23

Table 11 Calculated data for MACOR experiments

Specimen #	Seweryn				Leguillon			GSED ($SED_{cr} = 0.079$)					
								Low			High		
	d_o^{low}	d_o^{high}	R_f^{low}	R_f^{high}	$A_1^{average}$	A_{1c}^{low}	A_{1c}^{high}	R_{mat}^{notch}	A_{1c}^{low}	SED_{low}^f	R_{mat}^{notch}	A_{1c}^{high}	SED_{high}^f
$M-6$	0.073	0.086	1.39	1.29	14.52	13.86	15.08	0.033	13.46	0.091	0.039	14.65	0.078
$M-7, 14, 23$	0.073	0.086	1.16	1.08	9.87	10.63	11.47	0.033	9.66	0.082	0.039	10.38	0.071
$M-8, 13, 22$	0.073	0.086	1.09	1.02	8.24	9.40	10.12	0.033	8.47	0.075	0.039	9.07	0.065
$M-9, 12, 21$	0.073	0.086	1.45	1.36	9.78	8.31	8.92	0.033	7.21	0.145	0.039	7.70	0.127
$M-10, 11, 20$	0.073	0.086	1.35	1.25	7.29	6.50	6.95	0.033	5.28	0.150	0.039	5.62	0.132

Table 12 Calculated data for experiments reported in Seweryn and Lukaszewicz (2002)

	Loading angle	Seweryn		Leguillon		GSED ($SED_{cr} = 1.601$)		
		d_o^{low}	R_f	A_1	A_{1c}	R_{mat}^{notch}	A_{1c}	SED^f
$\omega = 340°$	$\psi = 15°$	0.087	1.10	16.98	15.26	0.032	14.50	1.77
	$\psi = 30°$	0.087	1.29	15.44	12.20	0.032	13.08	2.23
	$\psi = 45°$	0.087	1.37	12.83	9.86	0.032	10.76	2.27
	$\psi = 60°$	0.087	1.38	9.49	7.45	0.032	7.68	2.44
	$\psi = 75°$	0.087	1.30	5.15	4.33	0.032	3.98	2.68
$\omega = 320°$	$\psi = 15°$	0.087	1.00	15.70	15.68	0.033	14.78	1.80
	$\psi = 30°$	0.087	1.05	15.07	14.84	0.033	14.00	1.72
	$\psi = 45°$	0.087	1.15	10.75	10.98	0.033	9.76	1.94
	$\psi = 60°$	0.087	1.08	9.49	7.45	0.033	7.68	2.44
	$\psi = 75°$	0.087	1.08	6.68	7.11	0.033	5.54	2.33

Table 12 continued

	Loading angle	Seweryn		Leguillon		GSED ($SED_{cr} = 1.601$)		
		d_o^{low}	R_f	A_1	A_{1c}	R_{mat}^{notch}	A_{1c}	SED^f
$\omega = 300°$	$\psi = 15°$	0.087	0.94	15.07	16.16	0.034	15.39	1.67
	$\psi = 30°$	0.087	1.01	14.83	15.80	0.034	15.02	1.64
	$\psi = 45°$	0.087	1.14	15.06	15.03	0.034	14.20	1.80
	$\psi = 60°$	0.087	0.99	12.11	13.42	0.034	12.37	1.53
	$\psi = 75°$	0.087	0.85	6.94	9.81	0.034	8.12	1.09
$\omega = 280°$	$\psi = 15°$	0.087	1.00	20.07	18.40	0.035	16.68	2.31
	$\psi = 30°$	0.087	0.88	17.63	18.23	0.035	16.53	1.82
	$\psi = 45°$	0.087	0.94	17.84	17.85	0.035	16.18	1.94
	$\psi = 60°$	0.087	0.90	14.59	16.82	0.035	15.41	1.43
	$\psi = 75°$	0.087	0.80	10.27	13.60	0.035	11.97	2.17

Table 13 Different values for α reported in literature and calculated by the GSED criterion

Material Ref	PMMA Banks and Arcan (1986)	PMMA Royer (1988)	PMMA Ueda et al. (1983)	PMMA Yuh and Shu (1997)	Al_2O_3 Fett et al. (1995)	Al_2O_3 Suresh et al. (1990)	Si_3N_4 Petrovic (1985)	PMMA b2	PMMA d	MACOR
α	0.887	0.891	0.74–0.78	0.898	0.78	0.96	0.79	0.550	0.592	0.632

References

Anderson T (2005) Fracture mechancis fundamentals and application. CRC Press

Banks L, Arcan M (1986) A compact mode II fracture specimen. American Soc Test Mater 7:347–363

Chang J, Xu J, Mutoh Y (2006) A general mixed mode brittle fracture criterion for cracked materials. Engrg Frac Mech 73:1249–1263

Dunn ML, Suwito W, Cunningham S (1997a) Fracture initiation at sharp notches: correlation using critical stress intensities. Int J Solids Struct 34(29):3873–3883

Dunn ML, Suwito W, Cunningham S, May CW (1997b) Fracture initiation at sharp notches under mode I, mode II, and mild mixed mode loading. Int J Fracture 84:367–381

Erdogan F, Sih G (1963) On the crack extention in plates under loading and transverse shear. J Basic Eng 85:519–527

Fett T (1996) Failure of brittle materials near stress singularities. Eng Fract Mech 53:511–518

Fett T, Gerteisen G, Hahnenberger S, Martin G, Munz D (1995) Fracture tests for ceramics under mode-I, mode-II and mixed mode loading. J Eur Ceramic Soc 15:307–312

Gomez F, Elices M (2003) Fracture of componenets with sharp V-shaped notches. Eng Frac Mech 70:1913–1927

Lazzarin P, Zmabardi R (2001) A finite-volume-energy based approach to predict the static and fatigue behavior of components with sharp V-shaped notches. Int J Frac 112:275–298

Leguillon D (2002) Strength or toughness? A criterion for crack onset at a notch. Eur J Mech-A/Solid 21:61–72

Novozhilov V (1969) On a necessary and sufficient criterion for brittle strength. J Appl Math Mech (Translation of PMM) 33(2):212–222

Nuismer R (1975) An energy release rate criterion for mixed mode fracture. Int J Frac 11(2):245–250

Palaniswamy K, Knuass W (1978) On the problem of crack extension in brittle solids under general loading. Mech Today 4:87–148

Petrovic J (1985) Mixed mode fracture of hot-pressed Si_3N_4. J Eur Ceramic Soc 68:348–355

Royer J (1988) Study of pure and mixed mode fracture of a brittle material. Exp Mech 28(4):382–387

Seweryn A (1994) Brittle fracture criterion for structures with sharp notches. Eng Frac Mech 47(5):673–681

Seweryn A, Lukaszewicz A (2002) Verification of brittle fracture criteria for elements with V-shaped notches. Eng Frac Mech 69:1487–1510

Sih G, Macdonald B (1974) Fracture mechanics applied to engineering problems - strain energy density fracture criterion. Eng Frac Mech 6:361–386

Suresh S, Shih C, Morrone A, O'Dowd N (1990) Mixed mode fracture toughness of ceramic materials. J Eur Ceramic Soc 73:1257–1267

Szabó BA, Babuška I (1991) Finite element analysis. John Wiley & Sons, New York

Ueda Y, Ikeda K, Tetsuya Y, Aoki M (1983) Characteristic of brittle fracture under general combined modes incuding those under bi-axial tensile loads. Exp Mech 18:1131–1158

Yosibash Z, Adan O, Shneck R, Atlas H (2003) Thermo-mechanical failure criterion at the micron scale in electronic devices. Int J Frac 122:47–64

Yosibash Z, Bussiba A, Gilad I (2004) Failure criteria for brittle elastic materials. Int J Frac 125(3-4):307–333

Yosibash Z, Priel E, Leguillon D (2006) A failure criterion for brittle elastic materials under mixed-mode loading. Int J Frac 141(1):291–312

Yuh J, Shu L (1997) On the failure of cracks under mixed mode loads. Int J Frac 87:201–223